Published in final edited form as:
Nat Genet. ; 44(8): 922–927. doi:10.1038/ng.2349.

Loss-of-function mutations in *TGFB2* cause a syndromic presentation of thoracic aortic aneurysm

Mark E. Lindsay[1,2,3,16], **Dorien Schepers**[4,16], **Nikhita Ajit Bolar**[4], **Jefferson Doyle**[3], **Elena Gallo**[3], **Justyna Fert-Bober**[5], **Marlies J.E. Kempers**[6,7], **Elliot K. Fishman**[8], **Yichun Chen**[3], **Loretha Myers**[3], **Djahita Bjeda**[3], **Gretchen Oswald**[3], **Abdullah F. Elias**[3], **Howard P. Levy**[3], **Britt-Marie Anderlid**[9,10,11], **Margaret H. Yang**[10,11], **Ernie M.H.F. Bongers**[6,7], **Janneke Timmermans**[12], **Alan C. Braverman**[13], **Natalie Canham**[14], **Geert R. Mortier**[4], **Han G. Brunner**[6,7], **Peter H. Byers**[10,11], **Jennifer Van Eyk**[5], **Lut Van Laer**[4], **Harry C. Dietz**[2,3,17], and **Bart L. Loeys**[4,6,7,15,17]

[1]Helen B. Taussig Children's Heart Center, Department of Pediatrics, Johns Hopkins University School of Medicine, Baltimore, MD 21205, USA [2]Howard Hughes Medical Institute, Baltimore, MD 21205, USA [3]McKusick-Nathans Institute of Genetic Medicine, Johns Hopkins University School of Medicine, Baltimore, MD 21205, USA [4]Center of Medical Genetics, Faculty of Medicine and Health Sciences, University of Antwerp and Antwerp University Hospital, Antwerp, Belgium [5]Department of Medicine, Division of Cardiology, Bayview Proteomics Center, Johns Hopkins University, Baltimore, MD, 21224, USA [6]Department of Human Genetics, Radboud University Nijmegen Medical Centre, Nijmegen, The Netherlands [7]Institute for Genetic and Metabolic Disorders, Radboud University Nijmegen Medical Centre, Nijmegen, The Netherlands [8]Russell H. Morgan Department of Radiology and Radiological Science, Johns Hopkins School of Medicine, Baltimore, MD 21205, USA [9]Department of Clinical Genetics, Karolinska Institute, Karolinska University Hospital, Stockholm, Sweden [10]Department of Pathology, University of Washington School of Medicine, Seattle, WA 98195, USA [11]Department of Genetics, University of Washington School of Medicine, Seattle, WA 98195, USA [12]Department of Cardiology, Radboud University Nijmegen Medical Center, Nijmegen, The Netherlands [13]Department of Medicine, Washington University School of Medicine, St. Louis, MO 63110, USA [14]Department of Clinical Genetics, North West Thames Regional Genetics Service, (Kennedy Galton Centre), Northwick Park Hospital, Watford Road, Harrow, HA1 3UJ, United Kingdom [15]Department of Pediatrics and Genetics, Ghent University, Ghent, Belgium

Abstract

Correspondence should be addressed to Bart L. Loeys M.D., Ph.D. Center of Medical Genetics, Faculty of Medicine and Health Sciences, University of Antwerp/Antwerp University Hospital, Prins Boudewijnlaan 43, 2650 Antwerp (Edegem), Belgium, +32(0)3/2759774, +32(0)3/2759722, Bart.Loeys@ua.ac.be.
[16]These authors contributed equally to this work
[17]These authors jointly directed this work

Author Contributions

M.E.L., H.C.D., D.S., L.V.L. and B.L.L. conceived of the study and designed all experiments. M.E.L., D.S., L.V.L., H.C.D. and B.L.L. wrote the manuscript. D.S., M.H.Y. and N.A.B. performed microarray experiments and mutation analysis. J.J.D. performed protein blotting experiments. E.G. performed RT-PCR analysis of mouse aortas. J.F.-B. and J.V.E. performed serum TGF-β ligand analysis. E.K.F. performed, interpreted and produced multidetector-computed tomography images. Y.C. performed animal husbandry, genotyping and aorta dissections. L.M. performed IHC on human and mouse samples. D.B. performed all mouse echocardiograms. M.J.E.K., G.O., B.-M.A., E.M.H.F.B., J.T., A.C.B., N.C., G.R.M., H.G.B. and P.H.B. contributed patient material and clinical and pedigree data and revised the manuscript. A.F.E. and H.P.L. contributed to the whole-exome sequencing initiative.

Competing Financial Interests

The authors declare no competing financial interests.

Loeys-Dietz syndrome (LDS) associates with a tissue signature for high transforming growth factor (TGF)-β signaling but is often caused by heterozygous mutations in genes encoding positive effectors of TGF-β signaling, including either subunit of the TGF-β receptor or SMAD3, thereby engendering controversy regarding the mechanism of disease. Here, we report heterozygous mutations or deletions in the gene encoding the TGF-β2 ligand for a phenotype within the LDS spectrum and show upregulation of TGF-β signaling in aortic tissue from affected individuals. Furthermore, haploinsufficient *Tgfb2*$^{+/-}$ mice have aortic root aneurysm and biochemical evidence of increased canonical and noncanonical TGF-b signaling. Mice that harbor both a mutant Marfan syndrome (MFS) allele (*Fbn1*$^{C1039G/+}$) and *Tgfb2* haploinsufficiency show increased TGF-β signaling and phenotypic worsening in association with normalization of TGF-β2 expression and high expression of TGF-β1. Taken together, these data support the hypothesis that compensatory autocrine and/or paracrine events contribute to the pathogenesis of TGF-β–mediated vasculopathies.

Keywords

Aortic aneurysm; Marfan; Loeys-Dietz; TGFβ signaling; Transforming growth factor beta 2

The TGF-β family comprises three cytokines that regulate multiple aspects of cellular behavior including, proliferation, differentiation, migration and specification of synthetic repertoire[1]. Postnatally, TGF-β activity is most closely linked to wound healing, productive modulation of the immune system and multiple pathological processes, including cancer progression and tissue fibrosis[2]. Fibrillin-1, encoded by *FBN1*, the gene product altered in Marfan syndrome (MFS)[3], binds to the latent complex of TGFβ and regulates the release of active molecules in the extracellular environment[4,5]. LDS is a syndromic presentation of aortic aneurysm that is most often caused by mutations in the genes that encode the subunits of the TGF-β receptor, *TGFBR1* and *TGFBR2*[6,7]. Mutations in *SMAD3*, which encodes an intracellular mediator of TGF-β signaling, have also been described in individuals with phenotypic manifestations of LDS[8]. Three TGFβ ligand isoforms exist in humans (TGFβ1, -β2, and -β3, encoded by separate genes, *TGFB1*, *TGFB2*, and *TGFB3*, respectively) but their relative contributions to aortic aneurysm in the context of connective tissue disorders has not been explored.

The precise role of TGFβ signaling in aneurysm progression remains controversial. On the one hand, analyses of the aortic wall obtained from patients and mouse models have consistently shown the signature of increased TGF-β signaling for MFS, LDS, cutis laxa with aneurysm, bicuspid aortic valve with aneurysm and isolated familial thoracic aortic aneurysm caused by mutations in smooth muscle cell contractile proteins[6,9–11]. This signature includes increased phosphorylation and nuclear translocation of the receptor activated SMAD proteins (SMAD2 and SMAD3), increased expression of TGF-β–responsive gene products (for example, collagen, connective tissue growth factor (CTGF) and plasminogen activator inhibitor-1) and/or increased activation of noncanonical TGF-β _signaling cascades (prominently including ERK1 and ERK2 (ERK1/2))[12]. In mouse models of MFS, antagonism of TGF-β signaling using either TGFβ neutralizing antibodies or angiotensin receptor blockers attenuates multisystem disease manifestations, including aortic aneurysm[11,13,14]. On the other hand, an intuitive consideration of the primary consequence of many disease-associated mutations suggests the potential for loss of TGFβ signaling[7]. For example, while fibrillins may contribute to negative regulation of TGFβ signaling by sequestering ligand, they can also positively regulate signaling by concentrating cytokine at sites of intended function[15]. Most LDS mutations involve substitution of conserved residues in the kinase domains of TGFβ receptor subunits and recombinant expression of receptors harboring LDS mutations in cells naïve for the corresponding

receptor subunit fails to support canonical (SMAD-dependent) TGFβ signaling[16]. At least some of the *SMAD3* mutations that cause LDS are expected to confer functional haploinsufficiency by virtue of an early premature termination codon that induces accelerated decay of mutant mRNA and thus reduce signaling efficiency[8]. Furthermore lineage-specific abrogation of TGFβ signaling can impair aortic wall homeostasis[17,18]. It has been our hypothesis that this apparent paradox could be reconciled if compensatory paracrine or autocrine events in response to a relative loss of TGFβ signaling potential leads to functional overshoot[19]. Here we describe identification and mechanistic characterization of a new gene for a syndromic aneurysm presentation within the LDS spectrum that lends validity to this pathogenic model.

We identified eight families with an autosomal dominant aortic aneurysm phenotype with variable clinical expression. Features shared with MFS and LDS include aortic aneurysm, pectus deformity, arachnodactyly, scoliosis, and skin striae. Features shared with LDS but not MFS include hypertelorism, bifid uvula, bicuspid aortic valve, arterial tortuosity, club feet, and thin skin with easy bruising (Table 1, Fig. 1, and Supplementary Table 1). Ectopia lentis was not observed. Microarray analysis in two patients with these features who also had mild developmental delay, revealed two unique, heterozygous *de novo* chromosomal microdeletions at 1q41 (Fig. 1&2A). The deletion in one proband measures 6.5 Mb (215.5 Mb – 222.1 Mb; GRCh37/hg19) and encompasses 20 genes, whereas the deletion in the other is only 3.5 Mb (216.6 Mb – 220.2 Mb). Both deletions include the *TGFB2* gene, which encodes transforming growth factor β2 (TGFβ2), making it an obvious candidate gene for this aneurysm phenotype with MFS- and LDS-like features. We subsequently sequenced all exons and intron-exon boundaries of the *TGFB2* gene in a cohort of 86 aneurysm patients (34% familial) who were negative for *FBN1* and *TGFBR1/2* mutations. We identified a total of six heterozygous mutations in *TGFB2*, including one nonsense mutation, three missense mutations and two intragenic deletions, one in-frame and one causing a frameshift (Fig. 2B and Supplementary Figure 1). The three missense mutations, p.Arg327Trp, p.Arg330Cys and p.Pro366His, resulted in the substitution of evolutionarily conserved residues (Fig. 2B) and were categorized as probably damaging by Polyphen[20], deleterious by SIFT[21] and disease-causing by MutationTaster[22]. In addition, these mutations were not observed in the 1000 Genomes Project[23] and were not present in over 10,000 exomes in the NHLBI (USA) Exome Variant Server. All participating affected individuals tested positive for their family-specific *TGFB2* mutation (Fig. 2C). Because we found two whole gene deletions in addition to two nonsense mutations predicted to lead to nonsense-mediated mRNA decay (p.Tyr99* and p.Tyr369Cysfs*26), we propose haploinsufficiency as the relevant mechanism.

In addition to aneurysm, individuals with LDS show arterial tortuosity with prominent involvement of the vertebral and carotid arteries[6,16]. Individuals with *TGFB2* mutations can have similar arterial tortuosity (Fig. 3a, subject 7:III-1). Aortic tissue taken at the time of surgery demonstrates elastic fiber fragmentation and increased collagen and proteoglycan deposition (Fig. 3B&C and Supplementary Figure 2), histopathologic findings reminiscent of both MFS and LDS[24]. Immunohistochemical (IHC) analysis of aortic tissue from patients 7:III-1 and 5:II-2 demonstrated increased TGFβ signaling, as evidenced by increased nuclear activation of SMAD2 and pSMAD3 proteins and increased expression of TGFβ responsive gene products including collagen and connective tissue growth factor CTGF (Fig. 3C&D and Supplementary Figure 2). Whereas total TGF-β2 expression in IHC analyses was similar in affected individuals and in controls, expression of TGF-β1 ligand was higher in affected individuals (Fig. 3d).

We next examined the effect of *Tgfb2* haploinsufficiency in gene-targeted mice. While homozygous knockout (*Tgfb2*$^{-/-}$) mice are known to show late embryonic lethality secondary to congenital heart disease[25], the phenotype of *Tgfb2*$^{+/-}$ mice was not reported in

detail. Patients with LDS develop aortic aneurysm in a characteristic anatomic distribution characterized by dilation of the aortic root at the level of the sinuses of Valsalva[6]. This pattern is similar in patients with MFS[26] and in MFS mice harboring a heterozygous fibrillin-1 mutation (*Fbn1*$^{+/C1039G}$)[27]. By 8 months of age, *Tgfb2*$^{+/-}$ mice showed dilation of the aortic annulus and root but the more distal ascending aortic dimensions were normal (Fig. 4A&B). These findings demonstrate that loss of function of a single allele of *Tgfb2* is sufficient to cause aortic root aneurysm. To interrogate the state of TGFβ signaling in *Tgfb2*$^{+/-}$ mice, we performed western blot analysis of protein lysates derived from proximal ascending aortic segments. Similar to the signaling perturbations seen in *Fbn1*$^{+/C1039G}$ mice[12,28], aortas from *Tgfb2*$^{+/-}$ mice showed increased phosphorylation of Smad2, Smad3, and Erk1/2, when compared to wild-type mice (Fig. 4C and Supplementary Figure 3).

We next assessed for genetic interaction between targeted *Tgfb2*$^{+/-}$ *and Fbn1*$^{+/C1039G}$ alleles. The latter is associated with high TGFβ signaling during periods of rapid aneurysm progression[11,12,29]. *Tgfb2*$^{+/-}$*:Fbn1*$^{+/C1039G}$ animals demonstrate normal body size and growth with normal blood pressure indices (Supplementary Figure 4). These double heterozygous mice show a significant increase in aortic root dimension when compared to either *Fbn1*$^{+/C1039G}$ or *Tgfb2*$^{+/-}$ mice, at 2 and 4 months of age (Fig. 5A). Aortic dilatation was specific to the aortic root, recapitulating the zone of predisposition seen in people with either MFS or LDS. Histological examination shows equivalent elastic fiber disorganization and increased collagen deposition within the medial compartment of the aortic wall in *Tgfb2*$^{+/-}$ and *Fbn1*$^{+/C1039G}$ animals; both findings were greatly accentuated in *Tgfb2*$^{+/-}$*: Fbn1*$^{+/C1039G}$ mice (Fig. 5B& Supplementary Figure 5). IHC revealed a graded increase in nuclear accumulation of pSmad2 in the aortic media, with a pronounced increase in *Tgfb2*$^{+/-}$*: Fbn1*$^{+/C1039G}$ compound aortas (Fig. 5C). Western blot analysis, which integrates the performance of all cell types within the aorta, showed a subtle but significant increase in pSmad2 levels in *Fbn1*$^{+/C1039G}$ and *Tgfb2*$^{+/-}$*: Fbn1*$^{+/C1039G}$ mice, but no increase in either pSmad3 or pERK1/2 at this early timepoint (4 months) (Supplementary Figure 5). Analysis of mRNA levels in the proximal aorta at 2 months of age revealed normal expression of *Tgfb2* and *Tgfb3* in all three mutant genotypes; *Tgfb2*$^{+/-}$*: Fbn1*$^{+/C1039G}$ mice uniquely showed increased expression of *Tgfb1* (Fig. 5D) recapitulating observations in the human aorta (Fig. 3C). This upregulation was ligand-specific as no significant changes in *Tgfbr1* or *Tgfbr2* expression were detected (Supplementary Figure 6). At 4 months of age both *Tgfb2*$^{+/-}$ and *Tgfb2*$^{+/-}$*: Fbn1*$^{+/C1039G}$ mice showed decreased Tgfb2 in the circulation when compared to wild type littermates, whereas this level was increased in *Fbn1*$^{+/C1039G}$ animals (Supplementary Figure 7). While there was a trend for increased circulating Tgfb1 in all three mutant genotypes, high intragroup variability was observed (Data not shown).

This study demonstrates that heterozygous mutations in the gene encoding TGFβ2 are sufficient to cause a syndromic presentation of thoracic aortic aneurysm in both people and mice. Given the substantial clinical and mechanistic overlap with LDS, categorizing this disorder within the LDS-spectrum should facilitate patient diagnosis and management.

The pathogenesis of the TGFβ vasculopathies seems complex. Whereas the previous finding of mutations affecting TGF-β receptor subunits and intracellular mediators underscored the primary role of this cytokine family in aneurysm initiation and/or progression, the paradoxical association of an unequivocal signature for increased TGF-β signaling in postnatal tissues with mutations that would intuitively impair signaling has engendered controversy regarding the mechanism for LDS spectrum disorders. Attainment of mechanistic insight has been slowed by the myriad of interactions and functions supported by TGFβ receptors and intracellular signaling mediators and by the extent of cross-talk with other signaling cascades. The recent demonstration that the cleft palate seen upon neural-crest specific silencing of TβRII in mice manifests a gain of p38 signaling that is mediated

by TGF-β2 and a disease-specific TβR1-TβR3 receptor complex represents an overt example of this complexity and the potential inadequacy of intuitive disease model predictions[30].

Although our findings regarding *TGFB2* haploinsufficiency and aneurysm represent yet another example of the same paradox, they may offer experimental opportunities to clarify the mechanism. In the absence of any primary perturbation of intracellular signaling machinery, model systems may be more tractable. One testable hypothesis that derives from our observations is that compensatory upregulation of TGF-β1 expression in the aorta contributes to aortic disease. Further studies will be needed to determine whether concomitant silencing of TGF-β1 can rescue the TGFβ2 deficiency state and if the apparent overshoot in compensation reflects the total level of all bioavailable TGF-β ligands or a specific detrimental consequence of upregulation of TGF-β1 in the aorta. Alternatively, low TGF-β signaling in restricted cell populations may be a critical determinant of postnatal disease progression, perhaps setting the stage for paracrine overdrive of adjacent cell types with a relative preservation of signaling potential. It is notable that increased TGF-β1 has been documented in the aorta in LDS spectrum patients with loss-of-function *SMAD3* mutations[8] and in the circulation of people and mice with MFS[31].

Our observed deleterious genetic interaction between a $Fbn1^{+/C1039G}$ mutation causing MFS and *Tgfb2* haploinsufficiency causing a LDS-spectrum disorder is both novel and informative. MFS is the most comprehensively studied TGFβ vasculopathy, with clear evidence in support of an increased signaling state including cellular and tissue signatures that normalize in association with phenotypic rescue upon administration of TGFβ or ERK antagonists. In this light, pathogenic models that singularly invoke decreased TGFβ signaling for LDS-spectrum disorders would be difficult to reconcile with the worsening of disease seen in $Tgfb2^{+/-}$*:* $Fbn1^{+/C1039G}$ animals. It seems notable that aortic root enlargement can be detected in $Fbn1^{+/C1039G}$ and $Tgfb2^{+/-}$*:* $Fbn1^{+/C1039G}$ mice at 2–4 months of age, before overt evidence for excessive Smad2/3 or ERK1/2 activation by western blot analysis. This may suggest that the average performance of all cells within an aortic segment (the parameter monitored by immunoblots) is less important than the presence of even small subpopulations of bad-acting (i.e. high signaling) cells. In keeping with this hypothesis, the specific ERK1/2 inhibitor RDEA-119 was able to completely suppress abnormal aortic growth in $Fbn1^{+/C1039G}$ mice even when its use was restricted to age groups that did not yet show increased pERK1/2 in the aortic wall by western analyses[12]. Full clarity on these issues will facilitate the development and testing of novel treatment strategies that may find broad application.

Online Methods

Subjects

Patients were recruited from the Connective Tissue Clinic at Johns Hopkins Hospital (H.C.D.), Radboud University Hospital/Antwerp University Hospital (B.L.L), University of Washington Medical Center (P.B.) and Karolinska Institute (B-M.A). All samples were collected in compliance with the Institutional Review Board at each respective institution. 86 samples were obtained from individuals with features of syndromic connective tissue abnormalities, including proximal aortic aneurysm, who did not fulfill the diagnostic criteria for MFS of the 2010 Ghent nosology and who had remained negative after *TGFBR1/2* or *FBN1* mutation analysis.

Mutation analysis – Copy Number variant analysis and Sanger sequencing

DNA was extracted using standard procedures. Microarray analysis was performed using the Illumina HumanCytoSNP12-V2.1 BeadChip (Illumina, San Diego, CA) using standard protocols for proband 1. Data analysis was performed with the CNV-Webstore. For proband 2, micro-array analysis was performed by an OGT 180 kb oligo-array. PCR primers and conditions can be found in Supplementary Table 2. PCR products were bidirectionally sequenced using the BigDye Terminator Cycle Sequencing kit (Applied Biosystems, Carlsbad, CA) and separated on an ABI 3130XL Genetic Analyzer (Applied Biosystems, Carlsbad, CA). Sequence comparison and numbering are based on Ensembl transcript ENST00000366929 or NCBI NM_001135599.2 in which the A-nucleotide of the start codon ATG is assigned as position +1.

Mice

All mice were cared for under strict compliance with the Animal Care and Use Committee of the Johns Hopkins University School of Medicine. *TGFβ2*$^{+/-}$ mice were purchased through Jackson Laboratories (Bar Harbor, ME) as heterozygotes. For tissue analysis, animals were euthanized through inhalational halothane (Sigma, St, Louis, MO). After laparotomy and thoracotomy the ventricles and attached aortas were injected with 20 cc of phosphate-buffered saline (PBS) pH 7.4 to flush blood from the vascular system prior to dissection. All experimental mice were maintained on a C57Bl/6J background with the exception of *TGFβ2*$^{+/-}$ mice, which show impaired fertility on pure backgrounds and are therefore maintained on a mixed background at Jackson Laboratory.

Histology

Latex was injected into the left ventricular apex under low pressure until it was visible in the femoral artery. Animals were then fixed in Formalin (10%) for 24 hours before transfer to 70% ethanol for dissection and storage. Aortas were then removed from the animals or dissected *in situ* for photography prior to paraffinization and sectioning (5 μM). Slides were produced for tissue staining or stained with standard stains including VVG (Verhoeff-Van Gieson), H&E (Hematoxylin-Eosin), or Masson's Trichrome for quantitative analysis. Aortic architecture score was rated by three blinded observers and graded on an arbitrary scale of 1 (indicating no breaks in the elastic fiber) to 5 (indicating diffuse fragmentation). Human aortic samples were stained with mouse anti-α-smooth muscle actin (Dako 1A4), rabbit anti-pSMAD2 (Millipore AB3849), rabbit anti-pSMAD3 (Epitome #1880-1), rabbit anti-CTGF (Abcam ab6992), mouse anti-TGFB1 (Abcam ab64715), or rabbit anti-TGFB2 (Abcam ab66045) per manufacturer's instructions.

Western Blotting

After euthanasia and flushing, the ascending aorta (aortic root to origin of the right brachiocephalic) and the descending thoracic aorta (from ductal ampulla to diaphragm) were dissected and flash frozen in liquid nitrogen prior to storage at −80°C until processing. Western blotting procedures were performed as previously described[12].

Echocardiograms

Nair hair removal cream was used on all mice the day prior to echocardiograms. All echocardiograms were performed on awake, unsedated mice using the Visualsonics Vevo660 imaging system and a 30 MHz transducer. The aorta was imaged using a standard parasternal long axis view. Dimensions from each animal represent averages of three separate measurements made on still frames in systole of the maximal internal diameter of the aortic valve annulus, aortic sinuses, sinotubular junction, or ascending aorta. One of several cardiologists blinded to genotype performed all imaging and measurements.

RT-PCR

Aortas were dissected as previously described, flushed in PBS and directly stored into TRIzol® (Invitrogen). RNA was extracted according to manufacturer's instruction and purified with RNeasy mini columns (Qiagen). An on-column DNAse digest (Qiagen) was performed prior to the clean-up step to eliminate residual genomic DNA. cDNA was generated using TaqMan® High Capacity cDNA Reverse Transcription reagents and Q-PCR was performed in triplicate with TaqMan® Universal PCR Master Mix, all from Applied Biosystems. The following pre-validated TaqMan® probes were used to detect specific TGFβ transcripts and control transcripts: Mm01178820_m1 (TGFβ1), Mm01321739_m1 (TGFβ2), Mm01307950_m1 (TGFβ3), Mm99999915_g1 (GAPDH). Relative quantification for each transcript was obtained by normalizing against *Gapdh* transcript abundance according to the formula 2^(−Ct)/2^(−Ct GAPDH).

Quantification of circulating free TGF-beta 1 and TGF beta-2 in mouse plasma

Enzyme-Linked ImmunoSorbent Assay (ELISA) DuoSet for TGF-beta 1 and TGF-beta 2 (TGF-beta 1 and TGF beta 2 concentrations were measured by antibody-based sandwich Enzyme-Linked Immunosorbent Assay (ELISA) using electrochemiluminescence platform (Meso Scale Discovery, Gaithersburg, Md). For TGFbeta 1, the assay procedure follows the manufacturer's recommendations with minor changes[31]. For TGF beta 2, a customer MSD-ELISA was developed using capture detecting antibodies from R&D (DuoSet TGF beta 2, R&D, Minneapolis, MN) and optimized by comparing various diluents on human standards in mouse plasma. All plasma samples were run in duplicate. The lowest level of detection (LLOD) for TGF-beta 1 was 367.0 pg/mL, for TGF-beta 2 was 649.0 pg/mL. Data are displayed as mean with error bar representing one standard deviation. Results were considered valid when percentile of recovery (expected concentration divided by calculated concentration multiplied by 100) of the standards/calibrators was 100 ±20%, the coefficient of variation was <20%, intra-assay coefficient of variation was <10%, and the inter-assay coefficient of variation was <20%.

Statistical Analysis

All values are expressed as means + 2 standard errors of the mean (2SEM). Student *t* tests were used to evaluate significance between groups, with a p-value of <0.05 considered statistically significant. All significance reporting is standardized to (*p<0.05, **p<0.01, †p<0.005, ††p<0.001).

Supplementary Material

Refer to Web version on PubMed Central for supplementary material.

Acknowledgments

This study was supported in part by funding from the Fund for Scientific Research, Flanders (Belgium) [G.0458.09; G.0221.12]; European Grant Fighting Aneurysmal Disease [EC-FP7]; the Special Research Fund of the Ghent University [BOF10/GOA/005]; the National Institutes of Health (RO1- AR41135 and PO1-AR049698 to HCD; 5RC1HL100021-02 to J.V.E., H.C.D.; Institutional Clinical and Translational Science Award 1U54RR023561-01A1 to J.V.E); the National Marfan Foundation; the Smilow Center for Marfan Syndrome Research; the Howard Hughes Medical Institute; the Freudmann Fund for Research in Ehlers Danlos Syndrome and Related Disorders; and the Baylor-Hopkins Center for Mendelian Genetics (1U54HG006542). B.L.L. is senior clinical investigator of the Fund for Scientific Research, Flanders (Belgium); N.A.B. is supported by the Aneurysmal Pathology Foundation; D.S. is supported by a PhD grant from the Agency for Innovation by Science and Technology (IWT); E.G. is supported by a fellowship from the Helen Hay Whitney Foundation; J.J.D. is supported by the McKusick Fellowship of the National Marfan Foundation; and M.E.L. is supported by an NHLBI K08 Award (HL107738-01) and by a Fellow-to-Faculty Award from the National Marfan Foundation.

References

1. Moustakas A, Heldin CH. The regulation of TGFbeta signal transduction. Development. 2009; 136:3699–3714. [PubMed: 19855013]
2. Rahimi RA, Leof EB. TGF-beta signaling: a tale of two responses. J Cell Biochem. 2007; 102:593–608. [PubMed: 17729308]
3. Dietz HC, et al. Marfan syndrome caused by a recurrent de novo missense mutation in the fibrillin gene. Nature. 1991; 352:337–339. [PubMed: 1852208]
4. Isogai Z, et al. Latent transforming growth factor beta-binding protein 1 interacts with fibrillin and is a microfibril-associated protein. J Biol Chem. 2003; 278:2750–2757. [PubMed: 12429738]
5. Chaudhry SS, et al. Fibrillin-1 regulates the bioavailability of TGFbeta1. J Cell Biol. 2007; 176:355–367. [PubMed: 17242066]
6. Loeys BL, et al. A syndrome of altered cardiovascular, craniofacial, neurocognitive and skeletal development caused by mutations in TGFBR1 or TGFBR2. Nat Genet. 2005; 37:275–281. [PubMed: 15731757]
7. Mizuguchi T, et al. Heterozygous TGFBR2 mutations in Marfan syndrome. Nat Genet. 2004; 36:855–860. [PubMed: 15235604]
8. van de Laar IM, et al. Mutations in SMAD3 cause a syndromic form of aortic aneurysms and dissections with early-onset osteoarthritis. Nat Genet. 2011; 43:121–126. [PubMed: 21217753]
9. Renard M, et al. Altered TGFbeta signaling and cardiovascular manifestations in patients with autosomal recessive cutis laxa type I caused by fibulin-4 deficiency. Eur J Hum Genet. 2010; 18:895–901. [PubMed: 20389311]
10. Gomez D, et al. Syndromic and non-syndromic aneurysms of the human ascending aorta share activation of the Smad2 pathway. J Pathol. 2009; 218:131–142. [PubMed: 19224541]
11. Habashi JP, et al. Losartan, an AT1 antagonist, prevents aortic aneurysm in a mouse model of Marfan syndrome. Science. 2006; 312:117–121. [PubMed: 16601194]
12. Holm TM, et al. Noncanonical TGFbeta signaling contributes to aortic aneurysm progression in Marfan syndrome mice. Science. 2011; 332:358–361. [PubMed: 21493862]
13. Cohn RD, et al. Angiotensin II type 1 receptor blockade attenuates TGF-beta-induced failure of muscle regeneration in multiple myopathic states. Nat Med. 2007; 13:204–210. [PubMed: 17237794]
14. Ng CM, et al. TGF-beta-dependent pathogenesis of mitral valve prolapse in a mouse model of Marfan syndrome. J Clin Invest. 2004; 114:1586–1592. [PubMed: 15546004]
15. Arteaga-Solis E, et al. Regulation of limb patterning by extracellular microfibrils. J Cell Biol. 2001; 154:275–281. [PubMed: 11470817]
16. Loeys BL, et al. Aneurysm syndromes caused by mutations in the TGF-beta receptor. N Engl J Med. 2006; 355:788–798. [PubMed: 16928994]
17. Choudhary B, et al. Absence of TGFbeta signaling in embryonic vascular smooth muscle leads to reduced lysyl oxidase expression, impaired elastogenesis, and aneurysm. Genesis. 2009; 47:115–121. [PubMed: 19165826]
18. Langlois D, et al. Conditional inactivation of TGF-beta type II receptor in smooth muscle cells and epicardium causes lethal aortic and cardiac defects. Transgenic Res. 2010; 19:1069–1082. [PubMed: 20213136]
19. Lindsay ME, Dietz HC. Lessons on the pathogenesis of aneurysm from heritable conditions. Nature. 2011; 473:308–316. [PubMed: 21593863]
20. Sunyaev S, et al. Prediction of deleterious human alleles. Hum Mol Genet. 2001; 10:591–597. [PubMed: 11230178]
21. Ng PC, Henikoff S. Predicting deleterious amino acid substitutions. Genome Res. 2001; 11:863–874. [PubMed: 11337480]
22. Schwarz JM, Rodelsperger C, Schuelke M, Seelow D. MutationTaster evaluates disease-causing potential of sequence alterations. Nat Methods. 2010; 7:575–576. [PubMed: 20676075]
23. Durbin, RMea. A map of human genome variation from population-scale sequencing. Nature. 2010; 467:1061–1073. [PubMed: 20981092]

24. Maleszewski JJ, Miller DV, Lu J, Dietz HC, Halushka MK. Histopathologic findings in ascending aortas from individuals with Loeys-Dietz syndrome (LDS). Am J Surg Pathol. 2009; 33:194–201. [PubMed: 18852674]

25. Bartram U, et al. Double-outlet right ventricle and overriding tricuspid valve reflect disturbances of looping, myocardialization, endocardial cushion differentiation, and apoptosis in TGF-beta(2)-knockout mice. Circulation. 2001; 103:2745–2752. [PubMed: 11390347]

26. McKusick V. The cardiovascular aspects of Marfan's syndrome: a heritable disorder of connective tissue. Circulation. 1955; 11:321–342. [PubMed: 14352380]

27. Judge DP, et al. Evidence for a critical contribution of haploinsufficiency in the complex pathogenesis of Marfan syndrome. J Clin Invest. 2004; 114:172–181. [PubMed: 15254584]

28. Habashi JP, et al. Angiotensin II type 2 receptor signaling attenuates aortic aneurysm in mice through ERK antagonism. Science. 2011; 332:361–365. [PubMed: 21493863]

29. Neptune ER, et al. Dysregulation of TGF-beta activation contributes to pathogenesis in Marfan syndrome. Nat Genet. 2003; 33:407–411. [PubMed: 12598898]

30. Iwata J, et al. Modulation of noncanonical TGF-beta signaling prevents cleft palate in Tgfbr2 mutant mice. J Clin Invest. 2012; 122:873–885. [PubMed: 22326956]

31. Matt P, et al. Circulating transforming growth factor-beta in Marfan syndrome. Circulation. 2009; 120:526–532. [PubMed: 19635970]

Figure 1. Phenotypic characteristics of patients with *TGFB2* mutation

Significant clinical features of individuals with *TGFB2* mutations include mild hypertelorism (widely spaced eyes; 1-II:1, 3-III:1 and 7-III:1), malar hypoplasia (flat cheek bones;1-II:1,3-III:1, 4-II:1 and 7-III:1), retrognathia (receding chin; 1-II:1, 3-III:1, 4-II:1 and 7-III:1), arachnodactyly (long fingers; 1-II:1 and 4-II:1), pectus excavatum (7-III:1), pes planus (flat feet; 1-II:1 and 3-III:1) and hammer toes (1-II:1). Permission to publish photographs was obtained from the affected individuals or their parents.

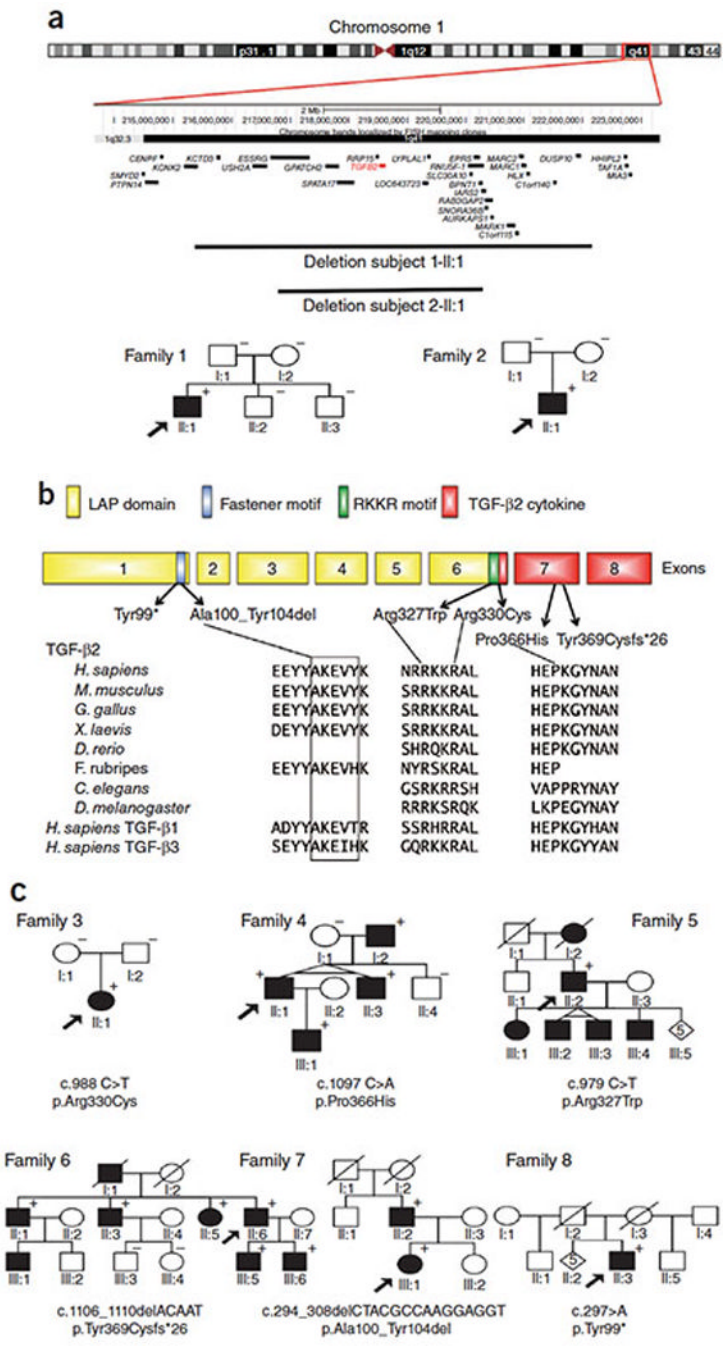

Figure 2. Mutational Analysis of *TGFB2* in aneurysm patients

(A.) Schematic representation of the microdeletions on chromosome 1q41. The *TGFB2* gene is indicated in red. Pedigrees for two patients with *de novo* chromosomal microdeleletions completely overlapping *TGFB2* (1-II:1 and 2-II:1) are shown. (+) Indicates presence of the described mutation in an associated individual while (−) indicates lack of mutation. (B-C.) *TGFB2* mutations and pedigrees for families 3–8. Pedigrees document an autosomal dominant pattern of inheritance. Mutations are annotated at the nucleotide (c.) and protein level (p.; three letter code for amino acids is used; reference transcript: Ensembl ENST00000366929 or NCBI NM_001135599.2). Circle, female; square, male; open symbol, unaffected; shaded symbol, affected; diagonal line, deceased. The location of

mutations in relation to the exons (numbers) of *TGFB2* and the domain organization is shown (LAP; latency associated peptide; RKKRA potential furin cleavage site). Evolutionary conservation of the mutated residues in *TGFB2* and related human cytokines (*TGFB1/3*) is shown.

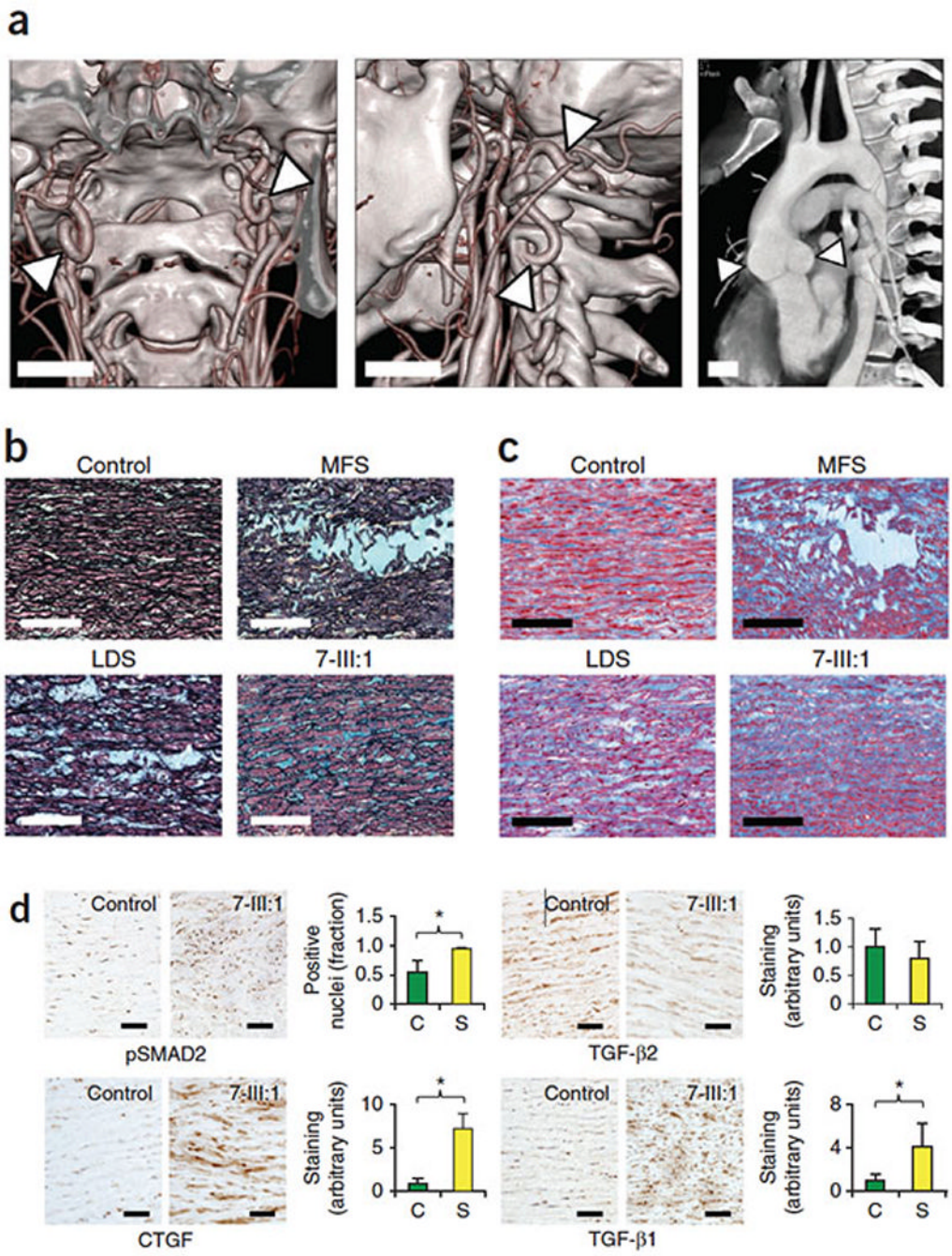

Figure 3. Cardiovascular Pathology in Human Subjects with *TGFB2* mutations

(A.) Multidetector computed tomography (MDCT) with 3 dimensional reconstruction of head and neck vessels demonstrating tortuosity of the distal cervical internal carotid arteries bilaterally (arrows, center panel) as well as the V1 segment of the left vertebral artery (arrows, left panel). MDCT imaging in modified sagittal view of dilated aorta at sinuses of Valsalva (arrows, right panel), Bars= 2 cm. (B.) Movat's pentachrome staining of human aortic samples demonstrating an increase in proteoglycan deposition (Blue staining in Movat's pentachrome) and elastic fragmentation (Black in Movat's pentachrome) in MFS, LDS, and patient with *TGFB2* mutation (7:III-1) versus control, Bar= 200μM, Enlargement Bar= 80μM. (C.) Masson's Trichrome staining of human aortic samples with increased

collagen deposition (Blue in Masson's Trichrome) in MFS, LDS, and patient with *TGFB2* mutation (7:III-1) versus control, Bar= 200μM, Enlargement Bar= 80μM. (D.) Immunocytochemical staining of the aortic media for phosphorylated Smad2 protein, CTGF, TGFB1, and TGFB2. Panels show control aorta (Control) and patient aorta with *TGFB2* mutation (7:III-1). Quantification of fraction of pSmad2 positive nuclei (pSMAD2) or staining (CTGF, TGFB1, TGFB2) represents staining of three control aortas (Co) versus patients 7:III-1 and 5:II-2 (Pts), Error bars equal 2 SEM, (*$p<0.05$). Bar= 80μM.

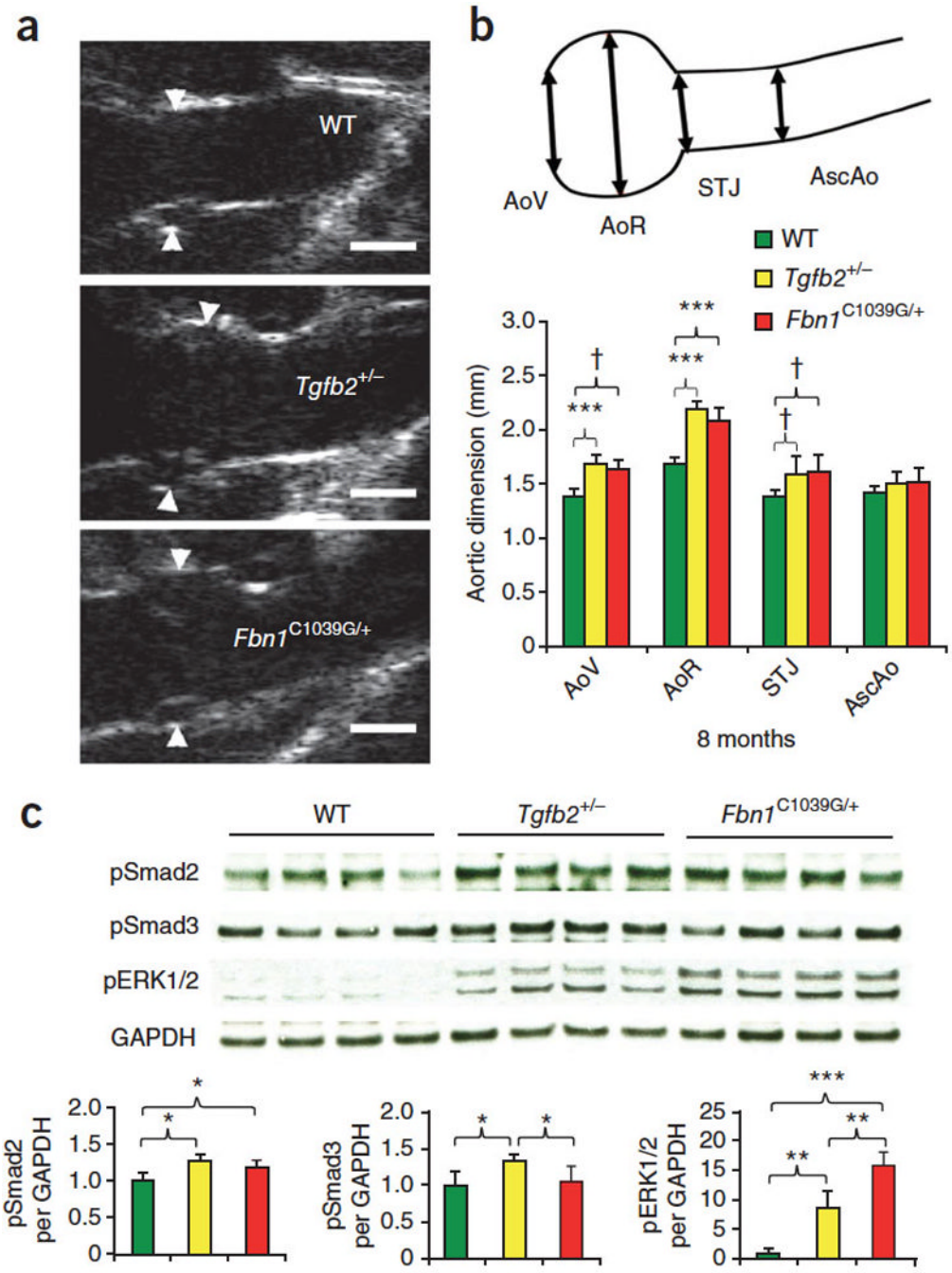

Figure 4. Haploinsufficiency for *Tgfb2* causes aortic root aneurysm in mice

(A.) Parasternal long axis echocardiographic systolic images of the aortic root of 8 month old wild type (n=10), *Tgfb2*$^{+/-}$ (n=6), and *Fbn1*$^{+/C1039G}$ mice (n=9). Arrows denote root dimension. Bar= 0.75 mm (B.) Echocardiographic quantification of dimensions at the aortic valve (AoV), aortic root (AoR), sinotubular junction (STJ), and ascending aorta (AscAo) in wild type, *Tgfb2*$^{+/-}$ and *Fbn1*$^{+/C1039G}$ mice at 8 months of age. (†p<0.005, †† p<0.001). There was no significant difference in aortic dimension between *Tgfb2*$^{+/-}$ and *Fbn1*$^{+/C1039G}$ mice at this age. (C.) Western blot analysis of murine ascending aortas demonstrating increased phosphorylation of Smad2, Smad3, and ERK proteins in 8 month old *Tgfb2*$^{+/-}$ and *Fbn1*$^{+/C1039G}$ mice. Graphs representing phosphoprotein western blot quantification

standardized to GAPDH expression, Error bars equal 2 SEM, (*p<0.05, **p<0.01, ††p<0.001).

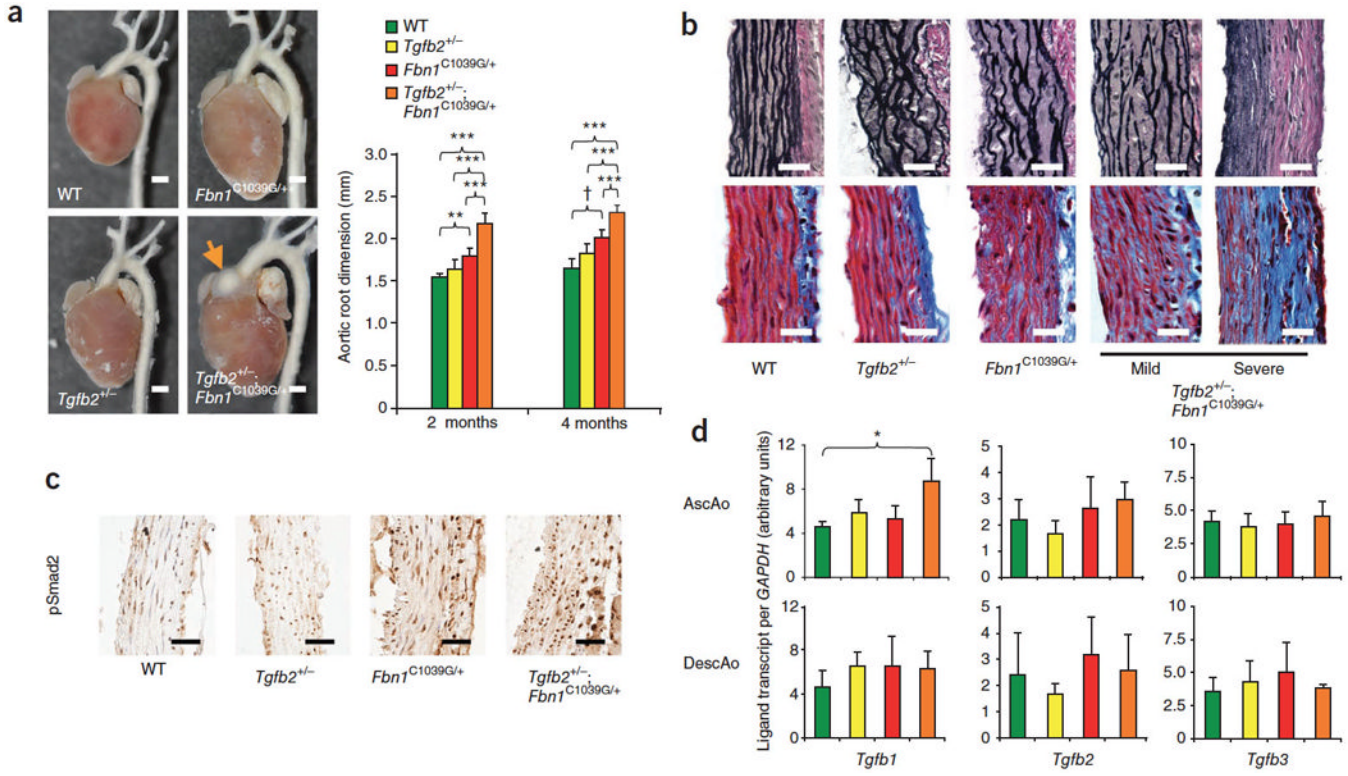

Figure 5. Synergistic pathology in *Tgfb2*$^{+/-}$:*Fbn1*$^{+/C1039G}$ double heterozygous mice

(A.) Photomicrographs and echocardiographic aortic root quantification of WT (n=8), *Tgfb2*$^{+/-}$ (n=8), *Fbn1*$^{+/C1039G}$ (n=7), and *Tgfb2*$^{+/-}$*: Fbn1*$^{+/C1039G}$ (n=11) mice. Orange arrow demonstrates a large sinus of Valsalva aneurysm. (**p<0.01, †p<0.005, ††p<0.001) Bar = 1.5 mm. (B.) Worsened aortic phenotype from *Tgfb2*$^{+/-}$*: Fbn1*$^{+/C1039G}$ double heterozygous mice. Panels of VVG (upper row) and Masson's Trichrome (bottom row) stained aortas from 4 month old mice demonstrating elastin fragmentation and increased collagen deposition in *Tgfb2*$^{+/-}$*: Fbn1*$^{+/C1039G}$ mice. Bar= 20 μm. (C.) Immunohistochemistry of phosphorylated Smad2 in aortas from 4 month old WT, *Tgfb2*$^{+/-}$, *Fbn1*$^{+/C1039G}$, and *Tgfb2*$^{+/-}$*: Fbn1*$^{+/C1039G}$ mice. Bar= 20 μm (D.) Transcript analysis of ascending and descending aortas of two month old WT (n=3), *Tgfb2*$^{+/-}$ (n=3), *Fbn1*$^{+/C1039G}$ (n=3), and *Tgfb2*$^{+/-}$*: Fbn1*$^{+/C1039G}$ (n=3) mice normalized to *GAPDH* expression, Error bars equal 2 SEM, (*p<0.05).

Table 1

Comparison of phenotypes in humans with *FBN1, TGFBR1, TGFBR2, SMAD3* or *TGFB2* mutations

	MFS	LDS		
	FBN1	***TGFBR1* or *TGFBR2***	***SMAD3***	***TGFB2***
Ectopia lentis	+++	−	−	−
Cleft palate/bifid uvula	−	++	+	+
Hypertelorism	−	++	+	+
Tall stature	+++	+	+	++
Arachnodactyly	+++	+	+	+
Pectus deformity	++	++	++	++
Club foot	−	++	+	++
Osteoarthritis	++	+	+++	+
Aortic root aneurysm	++	++	++	++
Early dissection	+	+++	++	+
Other aneurysm	+	++	++	+
Arterial tortuosity	−	++	++	+
BAV	−	++	+	+
Striae	++	+	+	+
Hernia	+	+	+	++
Dural ectasia	+	+	+	+

BAV, bicuspid aortic valve; −, absent or at population frequency; +, observed; ++, common; +++, typical.